KSCE Journal of Civil Engineering (2018) 22(1):101-109
DOI 10.1007/s12205-017-0654-2

Geotechnical Engineering
pISSN 1226-7988, eISSN 1976-3808
www.springer.com/12205

A Rapid Field Measurement Method for the Determination of Joint Roughness Coefficient of Large Rock Joint Surfaces

Rui Yong*, Xi Fu, Man Huang***, Qifeng Liang****, and Shi-Gui Du*****

Received March 2, 2016/Revised December 6, 2016/Accepted January 1, 2017/Published Online May 19, 2017

Abstract

An accurate measurement of the Joint Roughness Coefficient (JRC) of large rock joints is essential for understanding the mechanical behavior and permeability characteristics of rock mass. Determining the surface roughness of rock joints in situ, however, is time-consuming and depends on sophisticated instruments. This study was carried out to develop a systematic method of measuring the JRC values of large joint roughness profiles. The roughness profiles were accurately recorded by a hand profilograph in the field and then digitized with flexibly adjusted sampling intervals by the grayscale image processing method. The digitized profiles were correlated closely with the original roughness profiles. A computerized approach for JRC quantitative evaluation was proposed based on the roughness amplitude/joint length relationship with JRC. The interval effect analysis showed that this method was effective for estimating the JRC values of different sized rock joints. This JRC measurement method has been successfully used in a case study of killas rock joints in Changshan City, P.R. China.

Keywords: *Joint Roughness Coefficient (JRC), roughness amplitude, grayscale image processing, rock joint*

1. Introduction

Properties of rock joints such as apertures, roughness, infill, and persistency significantly affect the hydraulic and mechanical behavior of jointed rock masses (Tang *et al.*, 2016; Yong *et al*., 2016). It is acknowledged that roughness influences the friction angle, the dilatancy and the peak shear strength of rock joints (Zhang *et al.*, 2014). Because of the anisotropy, scale dependency, and the homogenous nature of rock joints, evaluating their surface roughness has become one of the most difficult problems in rock engineering over the years (Du, 1999; Kwon *et al*., 2010; Jang *et al.*, 2014; Ye *et al*., 2016).

Thus, considerable efforts have been made to quantify rock joint surface roughness using a variety of parameters and mathematical expressions (Tse and Cruden, 1979; Maerz *et al*., 1990; Kulatilake *et al*., 1999; Grasselli *et al.*, 2002; Tatone and Grasselli, 2010; Hong *et al*., 2014; Gao and Wong, 2015). Barton and Choubey (1977) proposed the Joint Roughness Coefficient (JRC), which has been widely used in evaluating the effect of roughness on rock joint shear strength in engineering practice (Maerz *et al.*, 1990; Gao and Wong, 2015). Several numerical approaches have been presented to facilitate the application of the JRC for surface roughness assessment in rock engineering practice over the past forty years (Yu and Vayssade, 1991). Also, fractal geometry theory has been utilized by researchers to characterize the roughness of joint profiles (Lee *et al.*, 1990; Hsiung *et al*., 1993; Yang *et al.*, 2001).

JRC values of rock joints vary from fracture to fracture and with the sample size (Jiang and Tanabashi, 2006). Recently, investigations have been performed on the sensitivity of joint surface roughness and the size of profiles, namely the scale effect (e.g., Bandis *et al.*, 1981; Xie *et al*., 1997; Fardin *et al*. (2001), and (2014); Tatone (2009); Tatone and Grasselli (2013); Ye *et al*., 2016). Swan and Zongqi (1985) observed the scale effect on the joint roughness by analyzing the root mean square of the surface profiles. Maerz *et al.* (1990) investigated the scale effect on both textural roughness and amplitude roughness parameters of two series of rock joint profiles using a shadow profilometry. Du *et al.* (2010) showed a negative scale effect existed in rock joint roughness by statistical analysis on asperity amplitudes. Most previous studies on surface roughness, and scale effects have tended to focus on samples within the size of 1 m^2 (Tatone and Grasselli, 2013). Large-scale joint profiles are rarely measured. Indeed, the roughness of field-scale profiles are often

*Lecturer, Dept. of Civil Engineering, Shaoxing University, Shaoxing 312000, P.R. China; Dept. of Civil Engineering, Queen's University, Kingston, Ontario K7L 3N6, Canada (E-mail: yongrui_usx@hotmail.com)
**Associate Professor, Dept. of Civil Engineering, Shaoxing University, Shaoxing 312000, P.R. China (E-mail: fuxi1984@hotmail.com)
***Associate Professor, Dept. of Civil Engineering, Shaoxing University, Shaoxing 312000, P.R. China (E-mail: hmcadx@126.com)
****Professor, Dept. of Civil Engineering, Shaoxing University, Shaoxing 312000, P.R. China (E-mail: qfliang@usx.edu.cn)
*****Professor, Dept. of Civil Engineering, Shaoxing University, Shaoxing 312000, P.R. China (Corresponding Author, E-mail: dsg@usx.edu.cn)

neglected in engineering practice where the size of natural joint surfaces may be several meters or even longer. Thus, it would seem worthwhile to determine joint roughness from large joint surface samples rather than small ones.

There are two major limitations in determining JRC of large joint surfaces. One is the measurement technique and the other is the JRC evaluation method. First, the measurement instruments should have sufficient accuracy, resolution, and ease of use in situ and in laboratory. If not, the roughness measurement may lack practical applicability, especially if the process is overly complex, excessively strict in measurement requirements, and limited by sample size. Recently, optical instruments are often utilized for measuring joint surfaces in-situ (Haneberg, 2007; Rousseau *et al.*, 2012; Feng *et al.*, 2013; Mah *et al.,* 2013; Ge *et al*., 2015). While these non-contact profiling methods have important features such as high speed of response and non-destructiveness measurement, their accuracy and precision are affected by soil or plant covering, light requirements, color-differences of rock components (Ge *et al.*, 2014). Furthermore, non-contact techniques are often costly, affecting their use by small businesses and individuals. Moreover, they are complicated and operationally challenging. As a result of these shortcomings, some researchers preferred to measure joint profiles by mechanical contour gauges (Kim *et al.*, 2013; Alameda-Hernández *et al.*, 2014; Morelli, 2014). Nevertheless, sample collection in the field is generally limited to small sized samples. Second, due to the disadvantage like labor-intensive and time-consuming, the methods for estimating the field-scale JRC values are seldom applied in the practice. As noted by Zhang *et al.* (2014), the JRC values must be scaled up by Barton's graphical solution on the basis of the roughness amplitude/joint length relationship with JRC. Yet visual inspection by this method is difficult and vulnerable to bias. Furthermore, the amplitude measurement using a second ruler or caliper is also time consuming and seldom applicable to JRC measurement in the practice.

In view of the limitations of the JRC evaluation method of large scale joint surfaces, three objectives were set for this study: (1) to present a quick and accurate method for measuring large rock joint surface profiles using flexibly sampling intervals; (2) to offer a computerized approach to JRC quantitative evaluation based on the roughness amplitude/joint length relationship with JRC proposed by Barton; and (3) to apply this method to JRC measurement and corresponding scale effects of rock joints in situ.

2. Measurement and Digitization of Rock Joint Roughness Profiles

The conventional contact profiling methods depend on direct contact with the actual measurement surface. These methods own significant merits like the ability for data accumulation and analysis, and the compatibility with previously accumulated measurement data (Du *et al.*, 2009). These measures are widely used in industry for research and development. However, the applicable apparatus for JRC measurement in the field, such as profile comb (Tatone and Grasselli, 2013) and the needle profilometer (Alameda-Hernández *et al*., 2014), fail to measure rock joints profiles several meters long. Consequently, a simple mechanical hand profilograph (Fig. 1) is suggested to measure the large scale rock joint profiles in the field. This profilograph has several components including feeler, drawing pen, balance block, fixed boards and drawing paper. The feeler is 80 mm long. One end is connected to the bottom of the balance block by a spring and the other end has a sharp steel needle. Mounted on the feeler point is a small, steel ball, which touches the joint surface during operation. The 20 mm long drawing pen is perpendicularly attached to the balance block. It can go up and down, depending on the joint surface, and is synchronized with the block's movement. The fixed stainless steel boards are used to hold the drawing paper and to provide an underlay. These boards are adjustable in length by a combination of two different layers (Fig. 2).

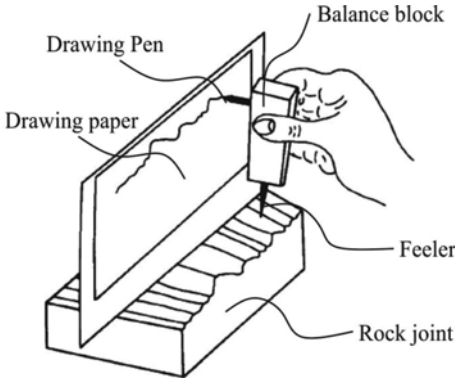

Fig. 1. A Schematic View of the Mechanical Hand Profilograph (Du, 1997)

Note that the planes of fixed boards and drawing paper are required to remain perpendicular to the rock joint surface during operation. Also, the feeler must be kept in constant contact with the rock joint surface so that the drawing pen can record the roughness profile on the board. In this way, a sudden jump in plotting is avoided if the rock joint profile mutation happens.

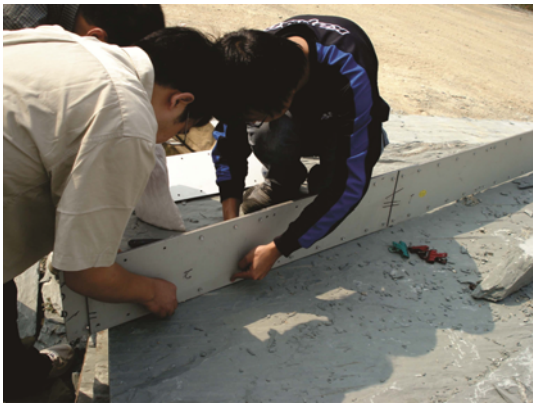

Fig. 2. Installation of the Fixed Boards for Measuring Field-scale Roughness Profiles

Another requirement is that the planes of the balance block and drawing pen board must be perpendicular to the plane of the fixed board.

The digitization of rock profiles can be recorded directly, but its accuracy depends on the instrument readings. Tatone and Grasselli (2010) re-digitized the ten standard profiles of rough rock joints by means of a profile combing technique using the horizontal point spacing of 0.5 mm and 1 mm. Yet data accuracy failed to be improved with smaller intervals, because the minimum distance of adjacent two points on the profile was limited to the comb's dimensional pin.

The roughness profiles can be digitized quantitatively according to the digital images of the profiles. Maerz *et al.* (1990) suggested a joint roughness measurement method using shadow profilometry. However, the images were not the true measurements of the rock profiles, and can be influenced by the variations in the angle of illumination, intensity of lighting, sensitivity of the camera and reflectivity of the rock. Jang *et al.* (2014) scanned the profiles and digitized the images by using Origin software at sampling intervals of 0.5 mm, 1.0 mm and 2.0 mm. Gao *et al.* (2015) used Barton's standard JRC profiles and acquired preliminary digital profiles for pixel analysis by MATLAB. But these researchers failed to give an available algorithm for searching the X-Y coordinates along the surface. Further, these image digitization methods have never been used for evaluating JRC values of field-scale rock joints. Because of these shortcomings, this present study used the grayscale image processing method for roughness profiles digitization. By so doing, the data obtained had a higher accuracy and was acquired by a more flexible sampling interval.

In photography and computing, a grayscale digital image carries intensive information. Each pixel in the image constitutes a single sample. Images of this sort, known as black and white, are composed exclusively of shades of gray, varying from black at the weakest intensity to white at the strongest. Barton's standard roughness profile of 16-18 was taken as an example (Fig. 3(a)). The profile curve was combined by different dark spots of varied shades. The first 1 cm length of this standard roughness profile is shown in the basic grayscale image (Fig. 3(b)). The relevant information of the imported file was extracted by MATLAB with the Image Processing Toolbox and saved in matrix form. As displayed in Fig. 3(c), it consists of 99 pixel grids; 9 pixels in width and 11 pixels in height. The intensity matrix is:

$$\begin{bmatrix} 254 & 255 & 244 & 255 & 255 & 242 & 255 & 255 & 252 \\ 255 & 255 & 254 & 255 & 251 & 252 & 250 & 248 & 124 \\ 255 & 249 & 255 & 237 & 250 & 255 & 13 & 0 & 2 \\ 254 & 253 & 255 & 255 & 255 & 0 & 0 & 7 & 6 \\ 128 & 64 & 0 & 0 & 0 & 11 & 7 & 0 & 4 \\ 0 & 4 & 3 & 9 & 0 & 0 & 0 & 1 & 0 \\ 5 & 0 & 7 & 0 & 7 & 0 & 8 & 1 & 1 \\ 3 & 0 & 9 & 0 & 198 & 249 & 255 & 251 & 253 \\ 255 & 0 & 249 & 255 & 238 & 255 & 255 & 242 & 254 \\ 252 & 253 & 255 & 239 & 255 & 244 & 249 & 255 & 252 \\ 252 & 255 & 247 & 245 & 255 & 255 & 251 & 252 & 255 \end{bmatrix} \quad (1)$$

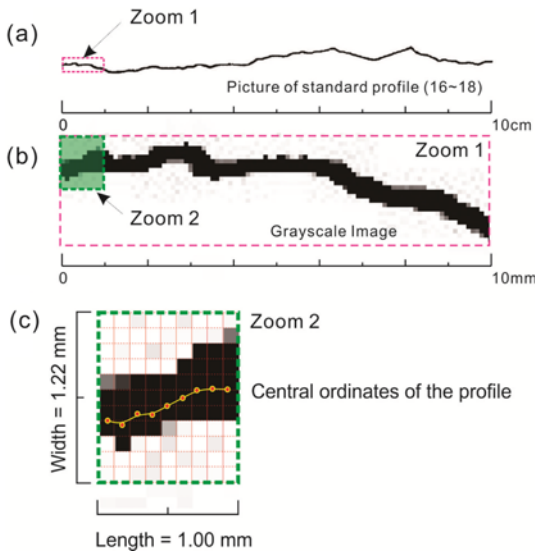

Fig. 3. Grayscale Data Extraction of 2D Profile from Barton Standard Roughness Profile: (1) Picture of Standard Profile 16~18, Resolution is 903 × 81 Pixels; (2) Zoom 1 which is the First 1 cm Length of (a) Magnified by 10 Times; Zoom 2 which is Grayscale Unit Image of the First 1 mm Length of (b)

Figure 3 Grayscale data extraction of 2D profile from Barton standard roughness profile: (1) picture of standard profile 16~18, resolution is 903×81 pixels; (2) zoom 1 which is the first 1cm length of (a) magnified by 10 times; zoom 2 which is grayscale unit image of the first 1mm length of (b).

The intensity of the grayscale image ranged from 0 to 255. A comparison of the intensity matrix with Fig. 3(c) showed a high correlation between cells of low intensity value and the center line of the profile curve. The columns C and rows R of grayscale matrix $I(i, j)$ represent the numbers of pixels in test width W and length L. The grayscale reflected the ordinate of the points on the surface profile and the intensity showed the proximity of each point to the center line of the profile. The abscissa of the points was calculated by the relationship between the grayscale columns and the profile length. The digitization accuracy ratio μ of the standard profile is written as:

$$\mu = \frac{L}{n} \quad (2)$$

Here, n represents the number of the grayscale columns in length L. In this example, the digitization accuracy ratio μ was 0.11 mm. The abscissa of each point is:

$$x_j = \mu \cdot (j - 1) \quad (3)$$

where j is the column of grayscale matrix I. The abscissas of the first 1mm length profile were 0.111 mm, 0.222 mm, 0.333 mm, 0.444 mm, 0.556 mm, 0.667 mm, 0.778 mm, 0.889 mm, 1.000 mm.

The ordinate of each point on the surface profile was calculated according to the following three steps,

a) A threshold s for removing the useless pixel values was set. If the intensity of the grayscale image was over the threshold s, the intensity values of the grayscale image were set to the same value as threshold. With the threshold at 100, the intensity matrix (1) is rewritten as:

$$\begin{bmatrix} 100 & 100 & 100 & 100 & 100 & 100 & 100 & 100 & 100 \\ 100 & 100 & 100 & 100 & 100 & 100 & 100 & 100 & 100 \\ 100 & 100 & 100 & 100 & 100 & 100 & 13 & 0 & 2 \\ 100 & 100 & 100 & 100 & 100 & 0 & 0 & 7 & 6 \\ 100 & 64 & 0 & 0 & 0 & 11 & 7 & 0 & 4 \\ 0 & 4 & 3 & 9 & 0 & 0 & 0 & 1 & 0 \\ 5 & 0 & 7 & 0 & 7 & 0 & 8 & 1 & 1 \\ 3 & 0 & 9 & 0 & 100 & 100 & 100 & 100 & 100 \\ 100 & 0 & 100 & 100 & 100 & 100 & 100 & 100 & 100 \\ 100 & 100 & 100 & 100 & 100 & 100 & 100 & 100 & 100 \\ 100 & 100 & 100 & 100 & 100 & 100 & 100 & 100 & 100 \end{bmatrix} \tag{4}$$

b) The weight w of the effective grayscale values was calculated,

$$w_{i,j} = 1 - \frac{I(i,j)}{s} \tag{5}$$

where i is the row of grayscale matrix I.

The weight matrix of intensity matrix (1) is:

$$\begin{bmatrix} 0 & 0 & 0 & 0 & 0 & 0 & 0 & 0 & 0 \\ 0 & 0 & 0 & 0 & 0 & 0 & 0 & 0 & 0 \\ 0 & 0 & 0 & 0 & 0 & 0 & 0.87 & 1 & 0.98 \\ 0 & 0 & 0 & 0 & 0 & 1 & 1 & 0.93 & 0.94 \\ 0 & 0.36 & 1 & 1 & 1 & 0.89 & 0.93 & 1 & 0.96 \\ 1 & 0.96 & 0.97 & 0.91 & 1 & 1 & 1 & 0.99 & 1 \\ 0.95 & 1 & 0.93 & 1 & 0.93 & 1 & 0.92 & 0.99 & 0.99 \\ 0.97 & 1 & 0.91 & 1 & 0 & 0 & 0 & 0 & 0 \\ 0 & 1 & 0 & 0 & 0 & 0 & 0 & 0 & 0 \\ 0 & 0 & 0 & 0 & 0 & 0 & 0 & 0 & 0 \\ 0 & 0 & 0 & 0 & 0 & 0 & 0 & 0 & 0 \end{bmatrix} \tag{6}$$

c) Searched for the central ordinate of the profile curve. The ordinate of each point is:

$$y_j = \mu \left(\frac{\sum_{i=1}^{R} i \times w_{i,j}}{\sum_{i=1}^{R} w_{i,j}} - \frac{\sum_{i=1}^{R} i \times w_{1,j}}{\sum_{i=1}^{R} w_{1,j}} \right) \tag{7}$$

The y values of the first 1 mm length profile were 0.000 mm, -0.035 mm, 0.059 mm, 0.053 mm, 0.113 mm, 0.164 mm, 0.219 mm, 0.220 mm, 0.219 mm.

The ordinate digitization process was simplified for joint surface roughness measurement in the field. Recorded the row i number of the effective grayscale in the matrix, whose intensity value was lower than threshold s. The average value a_i in these row numbers was obtained to determine the central point of the profile curve. The ordinate of each point is:

$$y_j = \mu \cdot (a_i - 1) \tag{8}$$

The y values of the first 1 mm length profile were 0.000 mm, 0.000 mm, 0.056 mm, 0.056 mm, 0.111 mm, 0.167 mm, 0.222 mm, 0.222 mm, 0.222 mm. This result were quite close to the ordinates calculated by Eq. (7). This simplified ordinate digitization process can satisfy the engineering application requirement.

To get the coordinates of the profile surface at the interval λ, the cubic spline interpolation was used to obtain $[x_j, y_j]$. Fig. 4. shows the digitized standard profile (16-18) at sampling intervals of 0.1 cm and 0.5 cm.

In previous research, the profile comb was used to digitize the roughness profile of rock joints. The measurement principle is shown in Fig. 5, and the coordinate interval of profiles was 0.5

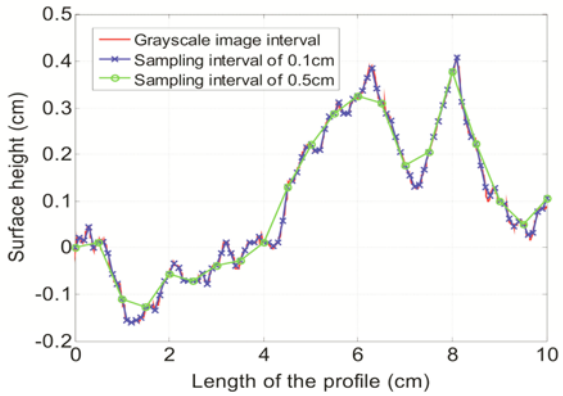

Fig. 4. Digitization of Standard Roughness Profile Under Different Sampling Intervals

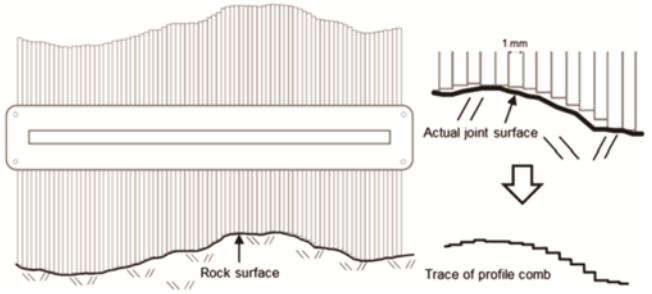

Fig. 5. Diagram Illustrating the use of a Profile Comb to Obtain 2D Profiles of a Rough Rock Joint (Tatone and Grasselli, 2010)

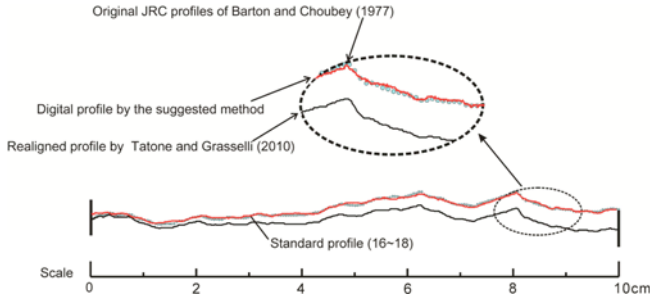

Fig. 6. Validation and Reproduction of the Standard Roughness Profile

mm. The maximum error of measurement was 3.8 mm (Fig. 6). Comparisons disclosed that the grayscale image processing method was more precise in fixed-point matching than the profile comb. The digitized profile correctly crossed the center points of the original standard profile and the measuring error was negligible at the level of approximately 0.1 mm.

3. Determination of JRC using Advanced Straight Edge Method

Since the sizes of the joint surface samples in the field are much larger than those in the laboratory, it is important to evaluate the JRC values of the former. Barton's graphical solution is widely used to determine the JRC values of field-scaled rock joins. However, the visual inspection is difficult and easily affected by artificial error. Furthermore, graphical solutions without the aid of computers are extremely tedious and awkward to implement.

Hu and Du (2008) investigated the concise formula of Barton's straight edge method based on the analysis of the geometrical characters of the chart. The JRC can be calculated as follows:

$$JRC_n = 400\frac{R_y}{L_n} \tag{9}$$

JRC_n is the joint roughness coefficient; R_y is the maximum amplitude of asperities (unit = cm) and L_n is the length of joint roughness profile (unit = cm).

Recording the maximum amplitude of asperities on large-scale joint profile traces is time consuming and therefore seldom used in practice for quantifying joint waviness (Fig. 7). According to the digitization procedure described previously, the programmed method for determining the amplitude of asperities is as follows:

Fig. 7. Method of Measuring Joint Trace Amplitude (Morelli, 2014)

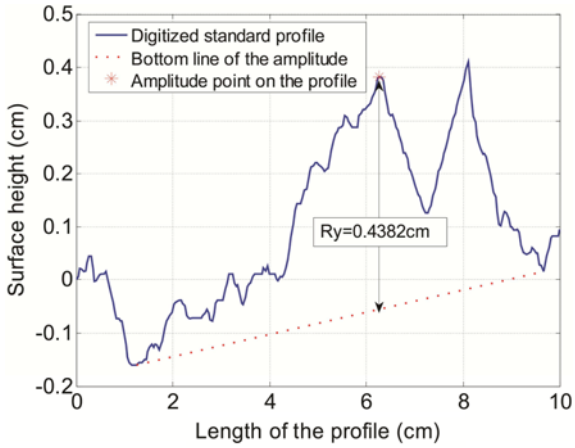

Fig. 8. The Amplitude of Asperities of the Standard Profile

a) Arbitrarily take two points from the digitized profile (x_p, y_p), (x_q, y_q):

b) The linear equation of the line passing through (x_p, y_p), (x_q, y_q) is:

$$\overline{y} = \frac{y_p - y_q}{x_p - x_q}(x - x_p) + y_p \tag{10}$$

c) Calculate the ordinate value $\overline{y_i}$ of the point x_i along the line from [x_p, x_q] and then calculate the difference R_i between $\overline{y_i}$ and y_i,

$$R_i = \frac{y_p - y_q}{x_p - x_q}(x_i - x_p) + y_p - y_i \; \overline{y_i} \tag{11}$$

where (x_i,y_i) is the coordinate of the digitized profile.

d) The amplitude of asperities R_y equals the maximum absolute value of R_i.

Based on the results, the joint roughness coefficient for Barton's straight edge method is as follows,

$$JRC_n = 400\frac{\max\left(\left|\frac{y_p - y_q}{x_p - x_q}(x_i - x_p) + y_p - y_i\right|\right)}{L_n} \tag{12}$$

A quality check was performed by measuring the JRC value of the standard profile in Fig. 2. The maximum amplitude R_y appeared at the length of 6.270 cm, with the value of 0.438 cm (Fig. 8). The JRC value estimated by Eq. (12) is 17.528. The value was well within the suggested JRC value range of 16-18.

4. Interval Effect on JRC Measurement

Previous research (Tse and Cruden, 1979; Yu and Vayssade, 1991; Hsiung *et al*., 1993; Tatone and Grasselli, 2010; Li and Zhang, 2015) found that the JRC values of joint roughness surfaces can be accurately well predicted by the geometrical parameter Z_2.

$$Z_2 = \frac{1}{L}\int_{x=0}^{x=L}\left(\frac{dy}{dx}\right)^2 \approx \left[\frac{1}{M(Dx)^2}\sum_{i=1}^{M}(y_{i+1} - y_i)^2\right]^{1/2} \tag{13}$$

Table 1. Summary of Suggested Relationships between Z2 and JRC of Previous Research Results

Author	Regression equation	Interval	Year
Tse R. and Cruden D.M.	$JRC = 32.2 + 32.47 \cdot \log_{10} Z_2$	1.27 mm	1979
Yu X.B. and Vayssade B.	$JRC = 60.31 \cdot Z_2 - 4.51$	0.25 mm	1991
	$JRC = 61.79 \cdot Z_2 - 3.47$	0.50 mm	
	$JRC = 64.22 \cdot Z_2 - 2.31$	1.00 mm	
Yang Z.Y., Lo S.C. and Di C.C.	$JRC = 32.69 + 32.98 \cdot \log_{10} Z_2$	0.50 mm	2001
Tatone Bryan S.A. and Grasselli G.	$JRC = 51.85(Z_2)^{0.60} - 10.37$	0.50 mm	2010
	$JRC = 55.03(Z_2)^{0.74} - 6.10$	1.00 mm	

where y is the amplitude of the roughness of the center line; x is the x-coordinates on the profile; L is the entire length of the profile; D_x is the equal interval; M is the number of intervals.

The suggested relationships are tabulated in Table 1 (Tse *et al.*, 1979; Yu *et al.*, 1991; Yang *et al.*, 2001; Tatone and Grasselli, 2010). However, these relationships were based on the back analyses of Barton's standard roughness profiles, which were limited to 10 cm. Also, none mentioned the effectiveness of the regression equations in large scale joint roughness measurement.

Barton's standard profiles (4-6) and (18-20) were taken as case studies to reveal the interval effect on JRC measurement. These six profiles were digitized using a sampling interval of 0.5 mm through the grayscale image processing method. The profiles are uniformly enlarged in both x and y direction. Enlargement, two and three times, of two 10 cm profiles are shown in Fig. 9. The JRC values of the profiles in length of 10 cm, 20 cm and 30 cm were calculated using the methods listed in Table 1. Table 2 shows that the JRC values of the 10 cm long profiles are within the JRC ranges suggested by Barton and Choubey (1977). The JRC values of the same shape profiles are increased by magnifying the sample's length.

Du and Hu (2009) examined rock joint roughness coefficients of different profiles by straight edge method and fractal dimension method. The profiles of larger sizes were magnified from the 10 cm long standard profile. The result revealed that magnified profiles had fractal similitude-self character and the JRC of rock joint was not affected by the sample sizes. In their study, a 10 cm long sample, with fractal dimension D = 1.0070 and JRC = 15, showed the same values after a magnification of 10 times. Ueng

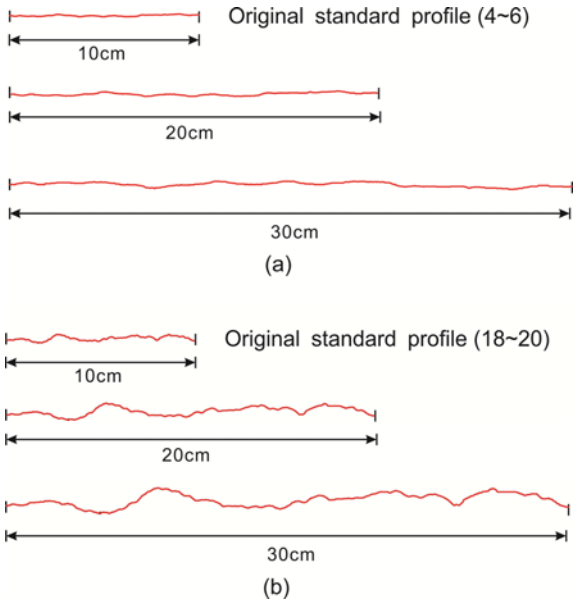

Fig. 9. Enlargement of Barton's Standard Profiles (a) JRC (4-6), (b) JRC (18-20)

et al. (2010) used a computer-aided manufacturing system to reproduce artificial rock joints for Barton's standard joint profiles of JRC (4-6) and JRC (18-20). Direct shear test results revealed that the enlarged joint specimens of 20 cm and 30 cm had almost the same peak shear strength as those of 10 cm long under similar normal stress conditions. Similar outcomes were also obtained by Ohnishi and Herda (1993). However, the observations

Table 2. Summary of the JRC Calculated Results using the Suggested Methods by Z_2

References no.	Length of 10 cm		Length of 20 cm		Length of 30 cm	
	(a)	(b)	(a)	(b)	(a)	(b)
Tse R. *et al.*	4.1897	18.3612	8.2301	19.7699	10.5772	20.8373
Yu X. B. *et al.*	5.0075	19.6888	7.8202	22.1217	9.8648	24.1341
Yang Z. Y. *et al.*	4.2397	18.6338	8.3436	20.0646	10.7275	21.1489
Tatone Bryan S. A. *et al.*	5.3755	18.4058	8.3290	20.1833	10.2928	21.6029

[(a)]JRC analysis results of enlargement of standard profile (4~6) with the interval of 0.5 mm; [(b)]JRC analysis results of enlargement of standard profile (18~20) with the interval of 0.5 mm.

in Table 2 show that the JRC values obviously varied with the profile length, even when the samples were same shape. Previous research has focused on the absolute sampling size while neglecting the relative size of the sampling interval. The different relative intervals d_x in large and small profiles resulted in conflicting results. In this study, the different sized profiles had the same sampling intervals of 0.5 mm. The profile length of 10 cm had a relative interval ratio $d_{10} = 0.5/1000 = 5 \times 10^{-4}$; the relative interval ratio of 20 cm was 2.5×10^{-4}; the relative interval ratio of 30 cm was 1.67×10^{-4}. Therefore, it would be inappropriate to evaluate the JRC values of the field-scale and laboratory small roughness profiles with the same relationships in Table 1.

The magnification of the profile was written as λ. Based on Eq. (12), the JRC value of the magnified profile was:

$$JRC_n(\lambda) = 400\frac{\max\left(\left|\frac{y_p - y_q}{x_p - x_q}(x_i - x_p)\cdot\lambda + (y_p - y_i)\cdot\lambda\right|\right)}{\lambda \cdot L_n} = JRC_n \tag{14}$$

As previously noted the JRC value would not be changed by enlarging the geometric size of the joint specimens. Thus, the method based on the roughness amplitude/joint length relationship with JRC was effective for estimating JRC of large scale rock joints.

5. Application of JRC Measurement of Large Scale Rock Joints in the Field

The steps in the rapid field method for measuring JRC values of large rock joint surfaces are shown in the following flowchart (Fig. 10).

A trial was performed on the natural rock joints located in Changshan City, Zhejiang Province, P.R. China. The main lithology of the joint wall is killas, which has the plate-type structure and the protolith is intermediate tufa. It is slightly weathered, integrated and structurally compact. The sample of this study case was 700 cm long, which was measured by the simple mechanical hand profilograph. The image of the recorded profile on the drawing paper was scanned by a high precision scanner "Colortrac SmartLF Gx + 42". The coordinate data of this profile was then obtained with a sampling interval of 1 mm based on the grayscale image processing method. Its digitized roughness profile is shown in Fig. 11. There is a comparison between the original image and digitized profile within the length of first 30 cm. It showed that the recorded joint profile by profilograph could be effectively transformed to the coordinate data for roughness analysis.

In order to study the scale dependency of joint surface roughness, samples of 10 cm, 20 cm, 30 cm, 40 cm, 50 cm, 60 cm, 70 cm, 80 cm, 90 cm, 100 cm, 150 cm, 200 cm, 250 cm, 300 cm, 350 cm, 400 cm, 450 cm, 500 cm, 550 cm, 600 cm, 650 cm and 700 cm were extracted from the digitized profile. The JRC

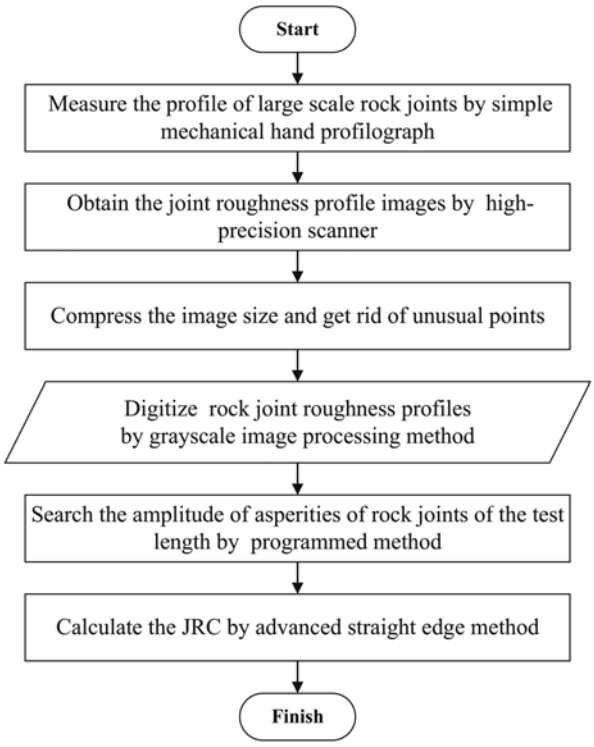

Fig. 10. Flowchart for Calculating the JRC of Field-scale Profiles in the Field

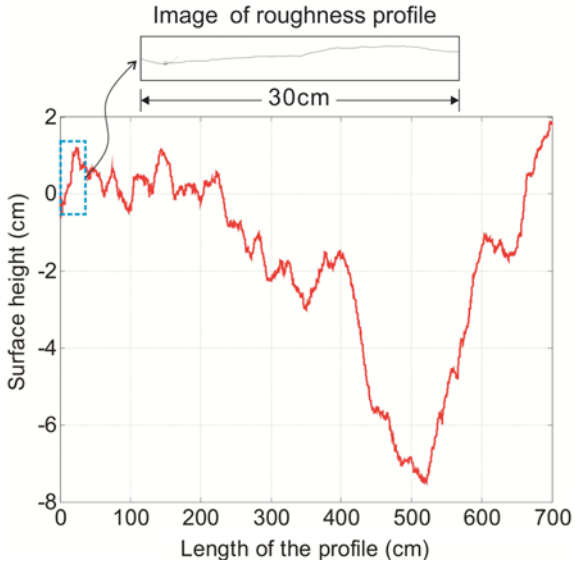

Fig. 11. Digitized Profile of Large Rock Joints in the Field

values were calculated by the advanced straight edge method and the results were plotted (see Fig. 12). The distribution of JRC values showed a negative scale effect on joint roughness, JRC values gradually decreased as the sampling length increased. The JRC values of different sized samples agreed with exponential association function, expressed as:

$$JRC_n = 3.683 + 18.245 \times 0.980^{l_n} \tag{15}$$

As shown in Fig. 12., JRC values of different sized rock joints

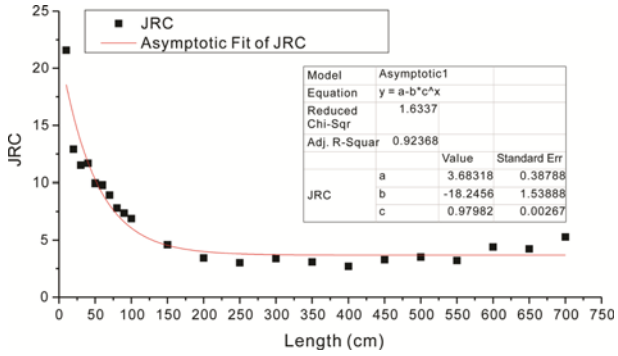

Fig. 12. Scale Effect on Rock Joints Roughness in the Field

are scale-dependent when the size of sample was small. When the sampling length is larger than 200 cm, the JRC values became almost constant.

6. Conclusions

One of the most challenging tasks in rock engineering is the in-situ measurement of rock joints and jointed rock mass properties. This study has shown the rapid field measurement method is useful for estimating the JRC value of the field-scale rock joints.

To meet the limitations of conventional contact profiling methods, a simple mechanical hand profilograph was used for recording roughness profiles several meters long. The instrument was convenient to carry and operate. The grayscale image processing method resulted in a high quality joint roughness profile digitization at flexibly adjusted sampling intervals. The data obtained demonstrated a better correlation with real rock joint profiles than those of the profile combing technique.

Based on the roughness amplitude/joint length relationship with JRC, a computerized approach was used to calculate the JRC values of large-scale rock joints. It is an improvement over the previous labor intensive and time consuming method for recording the maximum amplitude of asperities on large scale joint profile traces. This study found that it was effective for estimating the JRC values of field scale rock joints. The results showed a negative scale effect on joint roughness. Moreover, the JRC values remained almost constant when the sample size was over 200 cm.

For future work, the comparative study between the rapid field method and operation profiling method (e.g. laser scanning) is proposed for verification of the accuracy and precision when measuring joint surfaces of different sizes and directions.

Acknowledgements

The study was funded by National Natural Science Foundation of China (Nos. 41502300, 41427802, 41172292, 41302257). The authors appreciate the help provided by Harkiran Kaur, who made the careful English language editing on this manuscript before submitting. We are grateful to Prof. Ron Hotchkiss for his help with checking the data description.

References

Alameda-Hernández, P., Jiménez-Perálvarez, J., Palenzuela, J. A., El Hamdouni, R., Irigaray, C., Cabrerizo, M. A., and Chacón, J. (2014). "Improvement of the JRC Calculation using different parameters obtained through a new survey method applied to rock discontinuities." *Rock Mechanics and Rock Engineering*, Vol. 47, No. 6, pp. 2047-2060, DOI: 10.1007/s00603-013-0532-2.

Barton, N. and Choubey, V. (1977). "The shear strength of rock joints in theory and practice." *Rock mechanics*, Vol. 10, Nos. 1-2, pp. 1-54, DOI: 10.1007/BF01261801.

Bandis, S., Lumsden, A., and Barton, N. (1981). "Experimental studies of scale effects on the shear behaviour of rock joints." *International journal of rock mechanics and mining sciences & geomechanics abstracts*, Vol. 18, pp. 1-21, DOI: 10.1016/0148-9062(81)90262-X.

Du, S. (1999). *Engineering behavior of discontinuities in rock mass*, Beijing: Seismological Publishers.

Du, S. (1997). "The practicability of fractal methods on estimating rock joint roughness coefficient." *Earth Science*, Vol. 22, No. 6, pp. 665-668. (in Chinese)

Du, S., Hu, Y., and Hu, X. (2009). "Measurement of joint roughness coefficient by using profilograph and roughness ruler." *Journal of Earth Science*, Vol. 20, pp. 890-896. (in Chinese)

Du, S. G., Hang, M., Luo, Z. Y., Jia, R. D. and Wang, Y. M. (2010). "Scale effect of undulation amplitude of rock joints." *Journal of Enigneering Geolog*, Vol. 18, pp. 47-52. (in Chinese)

Fardin, N., Stephansson, O., and Jing, L. (2001). "The scale dependence of rock joint surface roughness." *International Journal of Rock Mechanics and Mining Sciences*, Vol. 38, No. 5, pp. 659-669, DOI: 10.1016/S1365-1609(01)00028-4.

Fardin, N., Feng, Q., and Stephansson, O. (2004). "Application of a new in situ 3D laser scanner to study the scale effect on the rock joint surface roughness." *International Journal of Rock Mechanics and Mining Sciences,* Vol. 41, No. 2, pp. 329-335, DOI: 10.1016/S1365-1609(03)00111-4.

Feng, Q., Fardin, N., Jing, L., and Stephansson, O. (2003). "A new method for in-situ non-contact roughness measurement of large rock fracture surfaces." *Rock Mechanics and Rock Engineering*, Vol. 36, No. 1, pp. 3-25, DOI: 10.1007/s00603-002-0033-1.

Gao, Y. and Wong, L. N. Y. (2015). "A modified correlation between roughness parameter Z2 and the JRC." *Rock Mechanics and Rock Engineering*, Vol. 48, No. 1, pp. 387-396, DOI: 10.1007/s00603-013-0505-5.

Ge, Y., Tang, H., Eldin, M. M. E., Chen, P., Wang, L., and Wang, J. (2015). "A Description for rock joint roughness based on terrestrial laser scanner and image analysis." *Scientific Reports*, Vol. 5, pp. 1-10, DOI: 10.1038/srep16999.

Ge, Y., Kulatilake, P. H., Tang, H., and Xiong, C. (2014). "Investigation of natural rock joint roughness." *Computers and Geotechnics*, Vol. 55, pp 290-305, DOI: 10.1016/j.compgeo.2013.09.015.

Grasselli, G., Wirth, J., and Egger, P. (2002). "Quantitative three-dimensional description of a rough surface and parameter evolution with shearing." *International Journal of Rock Mechanics and Mining Sciences*, Vol. 39, No. 6, pp. 789-800, DOI: 10.1016/S1365-1609(02)00070-9.

Haneberg, W. C. (2007). *Directional roughness profiles from three-dimensional photogrammetric or laser scanner point clouds*. In E.

Eberhardt, D. Stead, &T. Morrison (eds.), Rock Mechanics: Meeting Society's Challenges and Demands.

Hong, E.-S., Lee, I.-M., Cho, G.-C. and Lee, S.-W. (2014). "New approach to quantifying rock joint roughness based on roughness mobilization characteristics." *KSCE Journal of Civil Engineering*, Vol. 18, No. 4, pp. 984-991, DOI: 10.1007/s12205-014-0333-5.

Hsiung, S. M., Ghosh, A., Ahola, M. P., and Chowdhury, A. H. (1993). "Assessment of conventional methodologies for joint roughness coefficient determination." *International Journal of Rock Mechanics and Mining Sciences & Geomechanics Abstracts*, Vol. 30, No. 7, pp. 825-829, DOI: 10.1016/0148-9062(93)90030-H.

Hu, X. and Du S. (2008). "Concise formula of Barton's straight edge method for joint roughness coefficient." *Journal of Engineering Geology*, Vol. 16, No. 02, pp. 196-200. (in Chinese)

Jang, H., Kang, S., and Jang, B. (2014). "Determination of joint roughness coefficients using roughness parameters." *Rock Mechanics and Rock Engineering*, Vol. 47, No. 6, pp. 2061-2073, DOI: 10.1007/s00603-013-0535-z.

Jiang, Y., Li, B., and Tanabashi, Y. (2006). "Estimating the relation between surface roughness and mechanical properties of rock joints." *International Journal of Rock Mechanics and Mining Sciences*, Vol. 43, No. 6, pp. 837-846, DOI: 10.1016/j.ijrmms.2005.11.013.

Kim, D. H., Gratchev, I., and Balasubramaniam, A. (2013). "Determination of Joint Roughness Coefficient (JRC) for slope stability analysis: A case study from the Gold Coast area, Australia." *Landslides*, Vol. 10, No. 5, pp. 657-664, DOI: 10.1007/s10346-013-0410-8.

Kwon, T.-H., Hong, E.-S., and Cho, G.-C. (2010) "Shear behavior of rectangular-shaped asperities in rock joints." *KSCE Journal of Civil Engineering*, Vol. 14, No. 3, pp. 323-332. DOI: 10.1007/s12205-010-0323-1.

Kulatilake, P. H. S. W., and Um, J. (1999). "Requirements for accurate quantification of self-affine roughness using the roughness–length method." *International Journal of Rock Mechanics and Mining Sciences*, Vol. 36, No. 1, pp. 5-18, DOI: 10.1007/BF01045716.

Lee, Y. H., Carr, J. R., Barr, D. J., and Haas, C. J. (1990). "The fractal dimension as a measure of the roughness of rock discontinuity profiles." *International Journal of Rock Mechanics and Mining Sciences & Geomechanics Abstracts*, Vol. 27, No. 6, pp. 453-464, DOI: 10.1016/0148-9062(90)90998-H.

Li, Y. and Zhang, Y. (2015). "Quantitative estimation of joint roughness coefficient using statistical parameters." *International Journal of Rock Mechanics and Mining Sciences*, Vol. 77, pp. 27-35, DOI: org/10.1016/j.ijrmms.2015.03.016.

Mah, J., Samson, C., McKinnon, S. D., and Thibodeau, D. (2013). "3D laser imaging for surface roughness analysis." *International Journal of Rock Mechanics and Mining Sciences*, Vol. 58, pp. 111-117, DOI: 10.1016/j.ijrmms.2012.08.001.

Maerz, N. H., Franklin, J. A., and Bennett, C. P. (1990). "Joint roughness measurement using shadow profilometry." *International Journal of Rock Mechanics and Mining Sciences & Geomechanics*, Vol. 27, No. 5, pp. 329-343, DOI:10.1016/0148-9062(90)92708-M.

Morelli, G. L. (2014). "On joint roughness: measurements and use in rock mass characterization." *Geotechnical and Geological Engineering*, Vol. 32, No. 2, pp. 345-362. DOI: 10.1007/s10706-013-9718-3.

Ohnishi, Y. and Herda, H. (1993). "Shear strength scale effect and the geometry of single and repeated rock joints." *Proceedings of the 2nd International Workshop on Scale Effects in Rock Masses*, pp. 167-173.

Rousseau, B., Rivard, P., Marache, A., Ballivy, G., and Riss, J. (2012). "Limitations of laser profilometry in measuring surface topography of polycrystalline rocks." *International Journal of Rock Mechanics and Mining Sciences*, Vol. 52, pp. 56-60, DOI: 10.1016/j.ijrmms.2012.03.003.

Swan, G. and Zongqi, S. (1985). "Prediction of shear behaviour of joints using profiles." *Rock Mechanics and Rock Engineering*, Vol. 18, No. 3, pp.183-212. DOI: 10.1007/BF01112506.

Tang, H., Yong, R., and Eldin, M. E. (2016). "Stability analysis of stratified rock slopes with spatially variable strength parameters: The case of Qianjiangping landslide." *Bulletin of Engineering Geology and the Environment*, pp.1-15, DOI: 10.1007/s10064-016-0876-4.

Tatone, B. S. A (2009). *Quantitative characterization of natural rock discontinuity roughness in-situ and in the laboratory*, ([Ph.D. thesis]), University of Toronto, Toronto, Canada.

Tatone, B. S. A. and Grasselli, G. (2010). "A new 2D discontinuity roughness parameter and its correlation with JRC." *International Journal of Rock Mechanics and Mining Sciences*, Vol. 47, No. 8, pp. 1391-1400, DOI: 10.1016/j.ijrmms.2010.06.006.

Tatone, B. S. A. and Grasselli, G. (2013). "An investigation of discontinuity roughness scale dependency using high-resolution surface measurements." *Rock Mechanics and Rock Engineering*, Vol. 46, No. 4, 657-681, DOI: 10.1007/s00603-012-0294-2.

Tse, R. and Cruden, D. (1979). "Estimating joint roughness coefficients." *International Journal of Rock Mechanics and Mining Sciences & Geomechanics*, Vol. 16, pp. 303-307, DOI: 10.1016/0148-9062(79)90241-9.

Ueng, T. S., Jou, Y. J., and Peng, I. H. (2010). "Scale effect on shear strength of computer-aided-manufactured joints." *Journal of Geoengineering*, Vol. 5, No. 2, pp. 29-37, DOI: 10.6310/jog.2010.5(2).

Xie, H., Wang, J. A., and Xie, W. H. (1997). "Fractal effects of surface roughness on the mechanical behavior of rock joints." *Chaos, Solitons & Fractals*, Vol. 8, No. 2, pp. 221-252, DOI: 10.1016/S0960-0779(96)00050-1.

Yang, Z. Y., Di, C. C., and Yen, K. C. (2001). "The effect of asperity order on the roughness of rock joints." *International Journal of Rock Mechanics and Mining Sciences*, Vol. 38, No. 5, pp. 745-752, DOI: 10.1016/S1365-1609(01)00032-6.

Ye, J., Yong, R., Liang, Q. F., Huang, M., and Du, S. G. (2016). "Neutrosophic functions of the joint roughness coefficient and the shear strength: A case study from the pyroclastic rock mass in shaoxing city, China." *Mathematical Problems in Engineering*, Vol. 2016, Article ID 4825709, pp. 1-9, DOI: 10.1155/2016/4825709.

Yong, R., Li, C.D., Ye, J., Huang, M., and Du, S. (2016). "Modified limiting equilibrium method for stability analysis of stratified rock slopes." *Mathematical Problems in Engineering*, Vol. 2016, Article ID 8381021, pp. 1-9, DOI: 10.1155/2016/8381021.

Yu, X. and Vayssade, B. (1991). "Joint profiles and their roughness parameters." *International Journal of Rock Mechanics and Mining Sciences & Geomechanics Abstracts*, Vol. 28, No. 4, pp. 333-336, DOI: 10.1016/0148-9062(91)90598-G.

Zhang, G., Karakus, M., Tang, H., and Zhang, L. (2014). "A new method estimating the 2D Joint Roughness Coefficient for discontinuity surfaces in rock masses." *International Journal of Rock Mechanics and Mining Sciences,* Vol. 72, pp. 191-198, DOI: 10.1016/j.ijrmms.2014.09.009.